

Power Spectrum Analysis of the ESP Galaxy Redshift Survey

E. Carretti,^{1,2*} C. Bertoni,^{3†} A. Messina,^{4‡} E. Zucca^{5§} and L. Guzzo^{6¶}

¹*Istituto Te.S.R.E., Via Gobetti 101, I-40129 Bologna, ITALY*

²*Dipartimento di Astronomia, Via Ranzani 1, I-40127 Bologna, ITALY*

³*Istituto di Radioastronomia, Via Gobetti 101, I-40129 Bologna, ITALY*

⁴*Dipartimento di Scienze dell'informazione, Via Mura Anteo Zamboni 7, I-40126 Bologna, ITALY*

⁵*Osservatorio Astronomico di Bologna, Via Ranzani 1, I-40127 Bologna, ITALY*

⁶*Osservatorio Astronomico di Brera, Via Bianchi 46, I-23807, Merate(LC), ITALY*

Accepted. Received; in original form

ABSTRACT

We measure the power spectrum of the galaxy distribution in the ESO Slice Project (ESP) galaxy redshift survey. We develop a technique to describe the survey window function analytically, and then deconvolve it from the measured power spectrum using a variant of the Lucy method. We test the whole deconvolution procedure on ESP mock catalogues drawn from large N-body simulations, and find that it is reliable for recovering the correct amplitude and shape of $P(k)$ at $k > 0.065 h \text{ Mpc}^{-1}$. In general, the technique is applicable to any survey composed by a collection of circular fields with arbitrary pattern on the sky, as typical of surveys based on fibre spectrographs. The estimated power spectrum has a well-defined power-law shape k^n with $n \simeq -2.2$ for $k \geq 0.2 h \text{ Mpc}^{-1}$, and a smooth bend to a flatter shape ($n \simeq -1.6$) for smaller k 's. The smallest wavenumber where a meaningful reconstruction can be performed, does not allow us to explore the range of scales where other power spectra seem to show a flattening and hints for a turnover. We also find by direct comparison of the Fourier transforms, that the estimate of the two-point correlation function $\xi(s)$ is much less sensitive to the effect of a problematic window function as that of the ESP, than the power spectrum. Comparison to other surveys, shows an excellent agreement with other estimates from blue-selected surveys. In particular, the ESP power spectrum is virtually indistinguishable from that of the Durham-UKST survey over the common range of k 's, an indirect confirmation of the quality of the deconvolution technique applied.

Key words: surveys – galaxies: distances and redshifts – (cosmology:) large-scale structure of the Universe

1 INTRODUCTION

The quantitative characterisation of the galaxy distribution is a major aim in the study of the large-scale structure of the Universe. During the last 20 years, several surveys of galaxy redshifts have shown that galaxies group in clusters and superclusters, drawing structures surrounding large voids (see e.g. Guzzo 1999 for a review). The power spec-

trum of the galaxy distribution provides a synthetic statistical description of the observed clustering that, under some assumptions on its relation to the matter power spectrum, represents an important test for different structure formation scenarios (e.g. Peacock 1997 and references therein). Indeed, under the assumption of Gaussian fluctuations, the power spectrum totally describes the statistical properties of the matter density field (e.g. Peebles 1980).

* carretti@tesre.bo.cnr.it

† bertoni@astbo1.bo.cnr.it

‡ messina@cs.unibo.it

§ zucca@bo.astro.it

¶ guzzo@merate.mi.astro.it

In recent years, several estimates of the galaxy power spectrum have been obtained using galaxy samples selected at different wavelengths: radio (Peacock & Nicholson 1991), infrared (Feldman, Kaiser & Peacock 1994, Fisher et al. 1993, Sutherland et al. 1999) and optical (Park et al. 1994,

da Costa et al. 1994, Tadros & Efstathiou 1996, Lin et al. 1996, Hoyle et al. 1999), to mention the most recent ones.

The ESO Slice Project redshift survey (ESP, Vettolani et al. 1997, 1998) is one of the two deepest wide-angle surveys currently available, inferior only to the larger Las Campanas Redshift Survey (LCRS, Shectman et al. 1996). During the last few years, it has produced a number of statistical results on the properties of optically-selected galaxies, as e.g. the luminosity function (Zucca et al. 1997) or the correlation function (Guzzo et al. 2000). The geometry of the ESP survey (a thin row of circular fields, resulting in an essentially 2D slice in space) is such that an estimate of the power spectrum from these data represents a true challenge. In this paper we present the results of a detailed analysis that overcomes these difficulties, obtaining an estimate of the power spectrum from the ESP redshift data. The technique developed here to cope with the specific geometry of the survey is potentially interesting also for application to other surveys consisting of separate patches on the sky, as it could be the case, for example, of preliminary sub-samples of the ongoing SDSS (Margon 1998) and 2dF (Colless 1998) surveys.

The outline of the paper is as follows. We shall first recall the main features of the ESP survey and the sample selection (section 2), then discuss the power spectrum estimator adopted for the analysis (section 3) and the numerical tests performed in order to check its validity range (section 4). We shall then present the estimated power spectrum (section 5) and its consistency with the correlation function (section 6), and then discuss it in comparison to the results from other surveys (section 7). Section 8 summarises the results obtained, drawing some conclusions.

2 THE ESO SLICE PROJECT

The ESO Slice Project galaxy redshift survey (ESP, Vettolani et al. 1997, 1998) was constructed between 1993 and 1996 to possibly fill the gap existing at the time between shallow, wide angle surveys as the CfA2, and very deep, one-dimensional pencil beams. The survey was designed in order to allow the sampling of volumes larger than the maximum sizes of known structures and an unbiased estimate of the luminosity function of field galaxies to very faint absolute magnitudes. The survey and the data catalogue are described in detail in Vettolani et al. (1997, 1998). Here we limit ourselves to a summary of the main features relevant for the present analysis.

The ESP survey (see Figures 1 and 2) extends over a strip of $\alpha \times \delta = 22^\circ \times 1^\circ$, plus a nearby area of $5^\circ \times 1^\circ$, five degrees west of the main strip, in the South Galactic Pole region ($22^\circ 30' \leq \alpha \leq 01^\circ 20'$, at a mean declination of $-40^\circ 15'$ (1950)). This region was covered with a regular grid of adjacent circular fields, with a diameter of 32 arcmin each, corresponding to the field of view of the multifibre spectrograph OPTOPUS (Avila et al. 1989) at the ESO 3.6m telescope. The total solid angle covered by the survey is 23.2 square degrees and its position on the sky was chosen in order to minimize galactic absorption ($-60^\circ \lesssim b^{\text{II}} \lesssim -75^\circ$). The target objects, with a limiting magnitude $b_J \leq 19.4$, were selected from the Edinburgh–Durham Southern Galaxy Catalogue (EDSGC, Heydon–Dumbleton et al. 1989). A total

of 4044 objects were observed, corresponding to $\sim 90\%$ of the parent photometric sample and selected to be a random subset of the total catalogue with respect to both magnitude and surface brightness. The total number of confirmed galaxies with reliable redshift measurement is 3342, while 493 objects turned out to be stars and 1 object is a quasar at redshift $z \sim 1.174$. No redshift measurement could be obtained for the remaining 208 spectra. About half of the ESP galaxies present spectra with emission lines. Particular attention was paid to the redshift quality and several checks were applied to the data, using also multiple observations of ~ 200 galaxies and ~ 750 galaxies for which the redshift from both absorption and emission line is available (Vettolani et al. 1998, Cappi et al. 1998). All details about the data reduction and sample completeness are reported in Vettolani et al. (1997, 1998).

Given the magnitude-limited nature of the survey, the computation of a clustering statistics like the power spectrum requires the knowledge of the selection function. This is defined as the expected probability to detect a galaxy at a redshift z and can be expressed as

$$s(z) = \frac{\int_{\max[L_1, L_{\min}(z)]}^{+\infty} \phi(L) dL}{\int_{L_1}^{+\infty} \phi(L) dL}, \quad (1)$$

where $\phi(L)$ is the luminosity function, L_1 is the minimum luminosity of the sample and $L_{\min}(z)$ is the minimum luminosity detectable at redshift z , given the sample limiting magnitude.

In the ESP survey the minimum luminosity corresponds to an absolute magnitude $M_{b_J,1} = -12.4 + 5 \log h$ (h is the Hubble constant in units of $100 \text{ km s}^{-1} \text{ Mpc}^{-1}$). $L_{\min}(z)$ is the luminosity of a galaxy at redshift z with an apparent magnitude equal to the apparent magnitude limit $b_J = 19.4$. The corresponding absolute magnitude is given by

$$b_J - M_{b_J} = 25 + 5 \log D_L(z) - K(z), \quad (2)$$

where D_L is the luminosity distance in Mpc and $K(z)$ is the K-correction. D_L is given by the Mattig formula (1958), which depends on the assumed cosmological model. For all ESP computations we assume a flat universe with $\Omega_o = 1$ and $\Lambda = 0$. Before proceeding to the computation of luminosity distances, we have converted the observed heliocentric redshifts in the catalogue to the Cosmic Microwave Background (CMB) rest frame using a standard procedure, as described in Carretti (1999). The luminosity distance is then given by

$$D_L(z) = 6000(1+z) \left(1 - \frac{1}{\sqrt{1+z}}\right) h^{-1} \text{Mpc}. \quad (3)$$

The K-correction is a function of the redshift z and of the morphological type of the galaxy. In order to apply the appropriate K-correction it is necessary to know the morphological type of each galaxy, which is not available. Following Zucca et al. (1997), we use an average K-correction, weighted over the expected morphological mixture at each z . See Zucca et al. (1997, cfr. their figure 1) for the details of this computation.

The luminosity function is such that $\phi(L)dL$ gives the density of galaxies with luminosity $L \in [L, L + dL]$. The ESP luminosity function is well approximated by a Schechter (1976) function (Zucca et al. 1997)

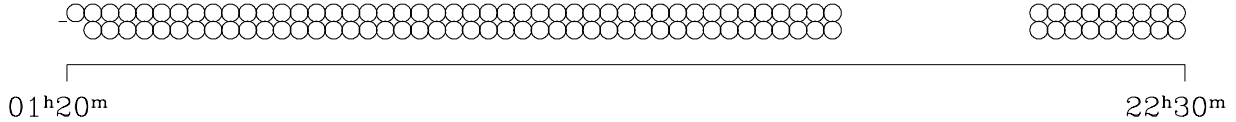


Figure 1. The area covered by the ESP survey on the sky consists of a set of 107 circular fields of $16'$ radius. As shown in this figure, they are arranged into 2 parallel rows and draw two thin slices over the celestial sphere of about $22^\circ \times 1^\circ$ and $5^\circ \times 1^\circ$ respectively, separated by $\sim 5^\circ$ (from Vettolani et al. 1997).

$$\phi(L)dL = \phi^* \left(\frac{L}{L^*} \right)^\alpha e^{-L/L^*} d\left(\frac{L}{L^*} \right) \quad (4)$$

with best fit parameters $\alpha = -1.22$, $M_{b,J}^* = -19.61 + 5 \log h$ and $\phi^* = 0.020 h^3 \text{ Mpc}^{-3}$. In reality, for $M_{b,J} > -16 + 5 \log h$ the faint end slope steepens with respect to the Schechter fit, and is better described by the addition of an extra power law. Nevertheless, this is relevant only for the very local part of the sample and a description of the selection function using a simple Schechter fit is perfectly adequate for our purposes.

Another quantity to be taken into account is the redshift completeness of the 107 fields, as not all target galaxies at the photometric limit were successfully measured. This can be expressed as (Vettolani et al. 1998)

$$C = \frac{N_Z}{N_T - N_S - 0.122 N_{NO}}, \quad (5)$$

where, for each field, N_T is the total number of objects in the photometric catalogue, N_Z is the number of reliable galaxy redshifts, N_{NO} is the number of not observed objects and N_S is the number of stars. In Figure 3 we plot the completeness values for each field. Field numbers < 100 denote fields in the northern row, while the others refer to the southern one.

The power spectrum analysis has been performed on both volume-limited and magnitude-limited catalogues. A volume-limited catalogue consists of all galaxies closer than a maximum redshift z_{max} and intrinsically more luminous than that specific value that would correspond to the apparent magnitude limit of the survey at the redshift z_{max} . In such a case, the expected mean density of galaxies does not vary with distance. A magnitude-limited catalogue, by definition, is simply a subset of all galaxies in the survey to a certain apparent magnitude, possibly with the addition of a distance cut at a maximum redshift z_{max} , to exclude the most distant part of the sample where the value of the selection function is dangerously close to zero. A magnitude-limited catalogue contains more objects than volume-limited ones, but the mean ensemble properties (as e.g. the galaxy luminosity distribution) vary with distance.

The comoving distance of a galaxy is given simply by

$$D_c(z) = \frac{1}{1+z} D_L(z) h^{-1} \text{Mpc}. \quad (6)$$

Table 1. Parameters of the samples extracted from the ESP survey: z_{max} is the maximum redshift, D_{max} the maximum distance in h^{-1} Mpc unit, M_{lim} the absolute magnitude limit for the volume-limited sample (we omit the $5 \log h$ term) and N is the galaxy number.

Sample	z_{max}	D_{max} (h^{-1} Mpc)	M_{lim}	N
ESPm523	0.20	523		3092
ESPm633	0.25	633		3306
ESP523	0.20	523	-20.1	481

The possible error introduced in the value of the comoving distances because of the uncertainty in the adopted cosmological model is less than 5% at a typical redshift $z = 0.20$, when the value of Ω_o is changed from 1 to 0.2.

We extract three samples from the ESP survey: two magnitude-limited and one volume-limited sample, as described in Table 1. The absolute magnitude limit of the latter is $M_{lim} = -20.1 + 5 \log h$ (hereafter we shall omit the $5 \log h$ term for simplicity).

3 POWER SPECTRUM ESTIMATOR

The galaxy power spectrum can be defined as

$$P(k) = \int \xi(x) e^{-i\mathbf{k} \cdot \mathbf{x}} d\mathbf{x}, \quad (7)$$

where $\xi(x)$ is the two-point correlation function, \mathbf{x} and \mathbf{k} are the comoving position and wavenumber vectors respectively, while $x = |\mathbf{x}|$ and $k = |\mathbf{k}|$. Under the hypothesis of homogeneity and isotropy, $P(k)$ and $\xi(x)$ are functions only of k and x respectively. By definition of the two-point correlation function can be also written

$$P(k) \propto |\hat{\delta}(k)|^2, \quad (8)$$

where $\hat{\delta}(\mathbf{k})$ is the Fourier transform of the density contrast of the galaxies.

In this paper we follow the Fourier notation

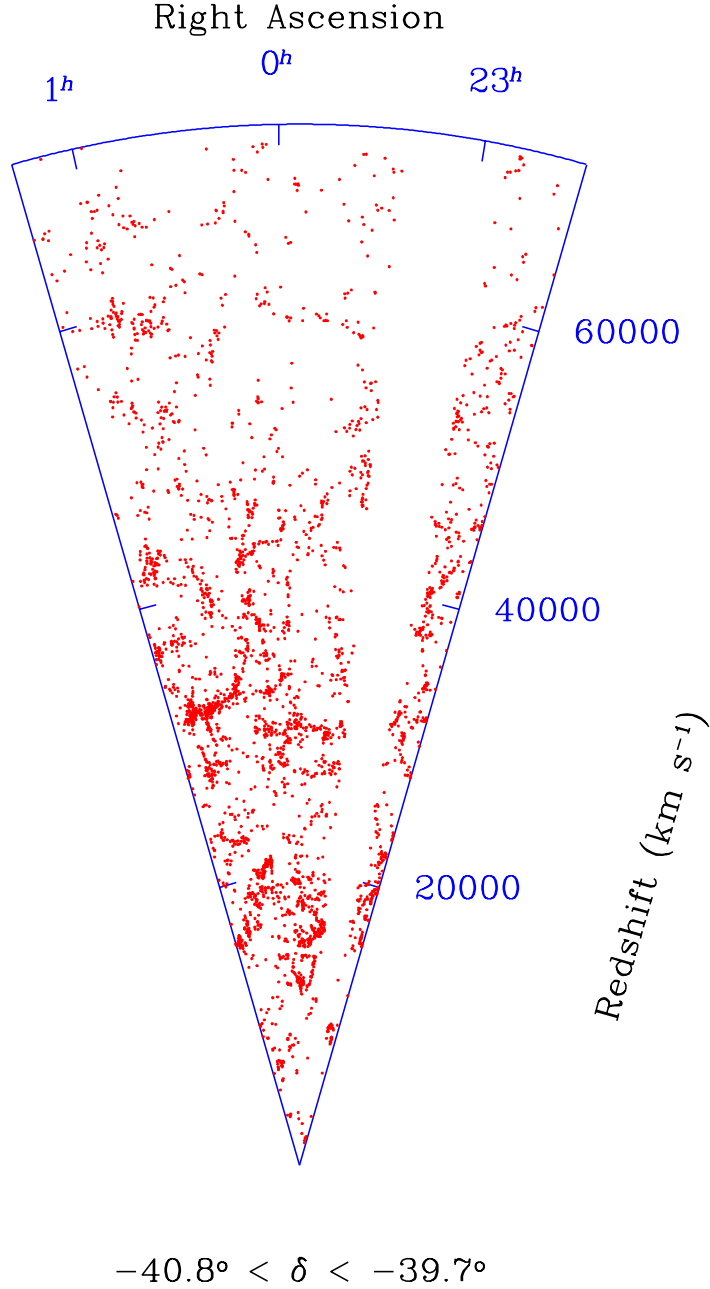


Figure 2. The galaxy distribution in the ESP redshift survey.

$$\hat{f}(\mathbf{k}) = \int f(\mathbf{x}) e^{-i\mathbf{k}\cdot\mathbf{x}} d\mathbf{x}, \quad (9)$$

$$f(\mathbf{x}) = \frac{1}{(2\pi)^3} \int \hat{f}(\mathbf{k}) e^{i\mathbf{k}\cdot\mathbf{x}} d\mathbf{k}. \quad (10)$$

To compute the power spectrum of galaxy density fluctuations from the observed galaxy distribution, we use a traditional Fourier method (cfr. Carretti 1999 for details), as developed by several authors (e. g. cfr. Peebles 1980, Fisher et al. 1993, Feldman et al. 1994, Park et al. 1994, Lin et al. 1996). We also apply a correction (Tegmark et al. 1998),

that accounts for our ignorance on the true value of the mean density of galaxies (Peacock & Nicholson 1991).

Given a sample of N galaxies of positions \mathbf{x}_j and weights w_j , an estimate of the density contrast Fourier transform is given by

$$\hat{\hat{\delta}}(\mathbf{k}) = \frac{V}{\sum_{j=1}^N w_j} \sum_{j=1}^N w_j e^{-i\mathbf{k}\cdot\mathbf{x}_j} - \hat{W}(\mathbf{k}), \quad (11)$$

where V is the volume of the sample and $\hat{W}(\mathbf{k})$ is the Fourier transform of the survey window function (hereafter a \sim will denote the quantities estimated from the data). The window

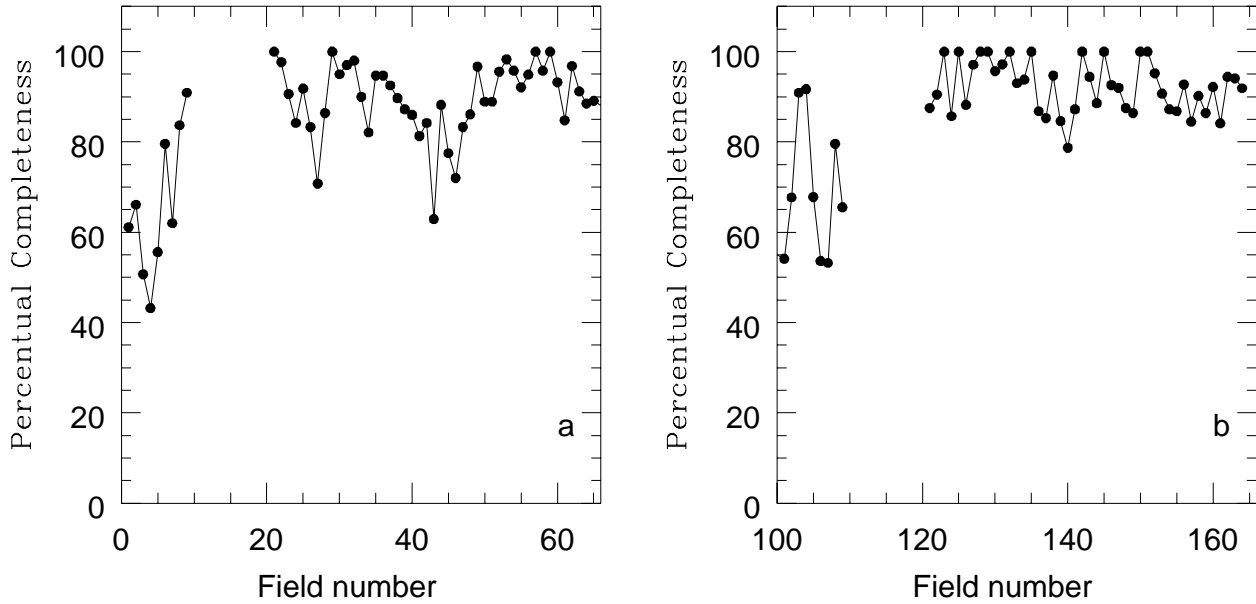


Figure 3. The redshift completeness within the ESP fields, i.e. the fraction of galaxies with measured redshift with respect to the total number of galaxies in the photometric sample in each field. Field numbers are as reported in the catalogue (Vettolani et al., 1998). The two panels are for the fields in the northern (a) and southern (b) rows respectively.

function $W(\mathbf{x})$ is 1 within the volume covered by the sample and 0 elsewhere, so it can be described as an ensemble of 107 cones. This geometry allows us to obtain analytically the Fourier transform $\hat{W}(\mathbf{k})$ as the sum of the Fourier transform of each cone. In equation 11 each galaxy contributes with some weight w_j . In a volume-limited catalogue all galaxies have equal weight and then

$$w_j = 1. \quad (12)$$

In a magnitude-limited catalogue the expected galaxy density decreases with the distance as described by the selection function. Thus the galaxy weight is the inverse of the selection function at its redshift z_j

$$w_j = \frac{1}{s(z_j)}. \quad (13)$$

If the catalogue completeness is $C < 1$, the previous weight should be modified as

$$w_j = \frac{1}{C(\mathbf{x}_j)} \quad (14)$$

for volume-limited catalogues, and as

$$w_j = \frac{1}{s(\mathbf{x}_j)C(\mathbf{x}_j)}, \quad (15)$$

for magnitude-limited catalogues. $C(\mathbf{x}_j)$ is the completeness of the sample at the position of the j^{th} galaxy.

Our adopted power spectrum estimator is defined with respect to $\tilde{\delta}(\mathbf{k})$ by the following equation (Tegmark et al. 1998)

$$\tilde{P}_c(\mathbf{k}) = \frac{|\hat{\delta}(\mathbf{k})|^2 - \tilde{b}(\mathbf{k})}{A(\mathbf{k})}, \quad (16)$$

where

$$A(\mathbf{k}) = \left(1 - \left| \frac{\hat{W}(\mathbf{k})}{\hat{W}(\mathbf{0})} \right|^2 \right) V \quad (17)$$

accounts for our ignorance of the mean galaxy density, while

$$\tilde{b}(\mathbf{k}) = \frac{V^2}{\left(\sum_{j=1}^N w_j \right)^2} \sum_{j=1}^N w_j^2 \left| e^{-i\mathbf{k} \cdot \mathbf{x}_j} - \frac{\hat{W}(\mathbf{k})}{\hat{W}(\mathbf{0})} \right|^2 \quad (18)$$

is the shot noise correction due to the finite size of the sample.

The observed power spectrum estimated by equation 16 is related to the true power spectrum $P(k)$ by

$$\tilde{P}_c(\mathbf{k}) = \frac{1}{(2\pi)^3 A(\mathbf{k})} \int P(k') \phi(\mathbf{k}, \mathbf{k}') d\mathbf{k}', \quad (19)$$

where

$$\phi(\mathbf{k}, \mathbf{k}') = \left| \hat{W}(\mathbf{k} - \mathbf{k}') - \frac{\hat{W}(\mathbf{k})}{\hat{W}(\mathbf{0})} \hat{W}(-\mathbf{k}') \right|^2. \quad (20)$$

For wavenumbers \mathbf{k} such that $|\hat{W}(\mathbf{k})| \ll |\hat{W}(\mathbf{0})|$ this equation reduces to the convolution between $P(k)$ and $|\hat{W}(\mathbf{k})|^2$.

To describe the convolved power spectrum we choose to average $\tilde{P}_c(\mathbf{k})$ over all directions

$$\tilde{P}_c(k) = \langle \tilde{P}_c(\mathbf{k}) \rangle \quad (21)$$

$$\begin{aligned}
&= \frac{1}{4\pi} \int_{\Omega_k} \tilde{P}_c(\mathbf{k}) d\Omega_k \\
&= \int_0^\infty k'^2 P(k') \chi(k, k') dk',
\end{aligned} \tag{22}$$

where Ω_k is the sphere defined by wavenumbers of amplitude k . The kernel of this integral equation is given by

$$\chi(k, k') = \frac{1}{2(2\pi)^4 V} \int_{\Omega_k} \int_{\Omega_{k'}} \psi(\mathbf{k}, \mathbf{k}') d\Omega_k d\Omega_{k'}, \tag{23}$$

where

$$\psi(\mathbf{k}, \mathbf{k}') = \frac{|\hat{W}(\mathbf{k} - \mathbf{k}') - \hat{W}(-\mathbf{k}') \hat{W}(\mathbf{k})/\hat{W}(\mathbf{0})|^2}{1 - |\hat{W}(\mathbf{k})/\hat{W}(\mathbf{0})|^2} \tag{24}$$

and $\Omega_{k'}$ is the sphere defined by wavenumbers of amplitude k' .

The strongly anisotropic geometry of the ESP survey introduces important convolution effects between the survey window function and the galaxy distribution. We have adopted the Lucy's deconvolution method (Lucy 1974; see also Baugh & Efstathiou 1993 and Lin et al. 1996, for a discussion about its application to power spectrum estimates), to clean the observed power spectrum for these effects.

The Lucy technique is a general method to estimate the frequency distribution $\psi(\eta)$ of a quantity η when we know the frequency distribution $\phi(y)$ of a second quantity y which is related to η by

$$\phi(y) = \int \psi(\eta) \Pi(y|\eta) d\eta, \tag{25}$$

where $\Pi(y|\eta) dy$ is the probability that $y' \in [y, y+dy]$ when $\eta' = \eta$. The probability $\Pi(y|\eta)$ must be known and the frequency distribution $\phi(y)$ is the observed one.

The solution of equation 25 can be obtained by an iterative procedure. Let $Q(\eta|y) d\eta$ be the probability that $\eta' \in [\eta, \eta+d\eta]$ when $y' = y$. The probability that $y' \in [y, y+dy]$ and $\eta' \in [\eta, \eta+d\eta]$ can be written as $\phi(y) dy Q(\eta|y) d\eta$ and $\psi(\eta) d\eta \Pi(y|\eta) dy$. From these two expressions and equation 25 we obtain

$$Q(\eta|y) = \frac{\psi(\eta) \Pi(y|\eta)}{\int \psi(\eta) \Pi(y|\eta) d\eta}, \tag{26}$$

which provides the identity

$$\psi(\eta) \equiv \int \phi(y) Q(\eta|y) dy. \tag{27}$$

The latter equation cannot be solved directly, since $Q(\eta|y)$ depends on the unknown $\psi(\eta)$ as well. Given a fiducial model for $\psi(\eta)$ and the known probability $\Pi(y|\eta)$, equation 26 provides an estimate for $Q(\eta|y)$. This estimate of Q and the identity 27 allows us to compute an improved estimate for $\psi(\eta)$. The process can then be repeated until convergency. In our specific case the equation to be solved is eq. 22, where $k'^2 \chi(k, k')$ plays the role of the probability $\Pi(y|\eta)$. If we sample k on logarithmic intervals the convolution integral becomes

$$\tilde{P}_c(k) = \int k'^3 P(k') \chi(k, k') \ln(10) d(\log_{10} k') \tag{28}$$

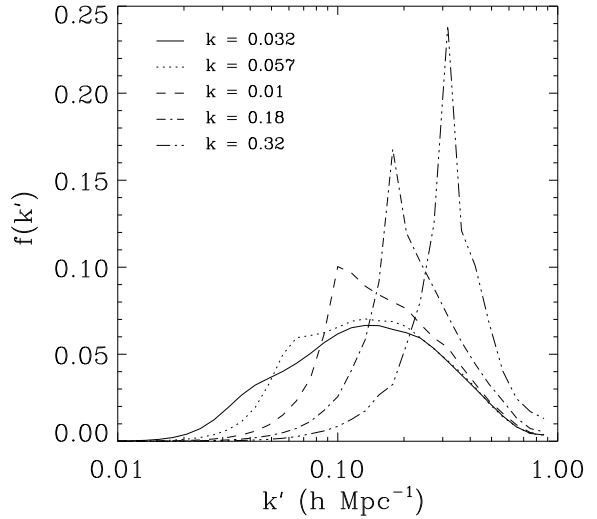


Figure 4. Behavior of the integrand of the convolution equation 28 normalized with respect to $\tilde{P}(k)$ for some k values. We plot the quantity $f(k') = k'^3 P(k') \chi(k, k') \ln(10) \Delta / \tilde{P}(k)$ for $(k = 0.032, 0.057, 0.1, 0.18, 0.32 h \text{ Mpc}^{-1})$, considering the kernel relative to the geometry of the $523 h^{-1} \text{ Mpc}$ sample.

and an iterative scheme for the deconvolved spectrum can be written as

$$\begin{aligned}
P^{m+1}(k_i) &= \frac{P^m(k_i)}{\sum_j \chi(k_j, k_i) \ln(10) \Delta} \\
&\cdot \sum_j \frac{\tilde{P}_c(k_j)}{\tilde{P}_c^m(k_j)} \chi(k_j, k_i) \ln(10) \Delta,
\end{aligned} \tag{29}$$

where

$$\tilde{P}_c^m(k_j) = \sum_r k_r^3 P(k_r) \chi(k_j, k_r) \ln(10) \Delta \tag{30}$$

and $\Delta = (\log_{10} k_{i+1} - \log_{10} k_i)$ is the logarithmic interval, while P^m denotes the m^{th} estimate of the spectrum.

One problem with the Lucy method is that of producing a more and more noisy solution as the iteration converges. To avoid this, Lucy suggests to stop the iteration after the first few steps. This is quite arbitrary and we prefer to follow Baugh & Efstathiou (1993; see also Lin et al. 1996) in applying a smoothing procedure at each step

$$P^m(k_i) = 0.25 P^m(k_{i-1}) + 0.5 P^m(k_i) + 0.25 P^m(k_{i+1}). \tag{31}$$

We use $P^0(k_i) = \text{constant}$ as initial guess for the power spectrum, but we checked that the solution is independent of the shape of $P^0(k_i)$. One consequence of this smoothing is that some degree of correlation is introduced among the bins of $P(k)$.

The importance of the convolution effects on different scales can be estimated by plotting the integrand of eq. (28) as a function of k' , for different values of k (Figure 4). If the window was a large and regular sample of the Universe, the plots would be sharply peaked at $k = k'$, as it actually happens for large values of k (small scales). On the other hand, for small values of k , i.e. for spatial wavelengths comparable to the typical scales of the window (which are quite small,

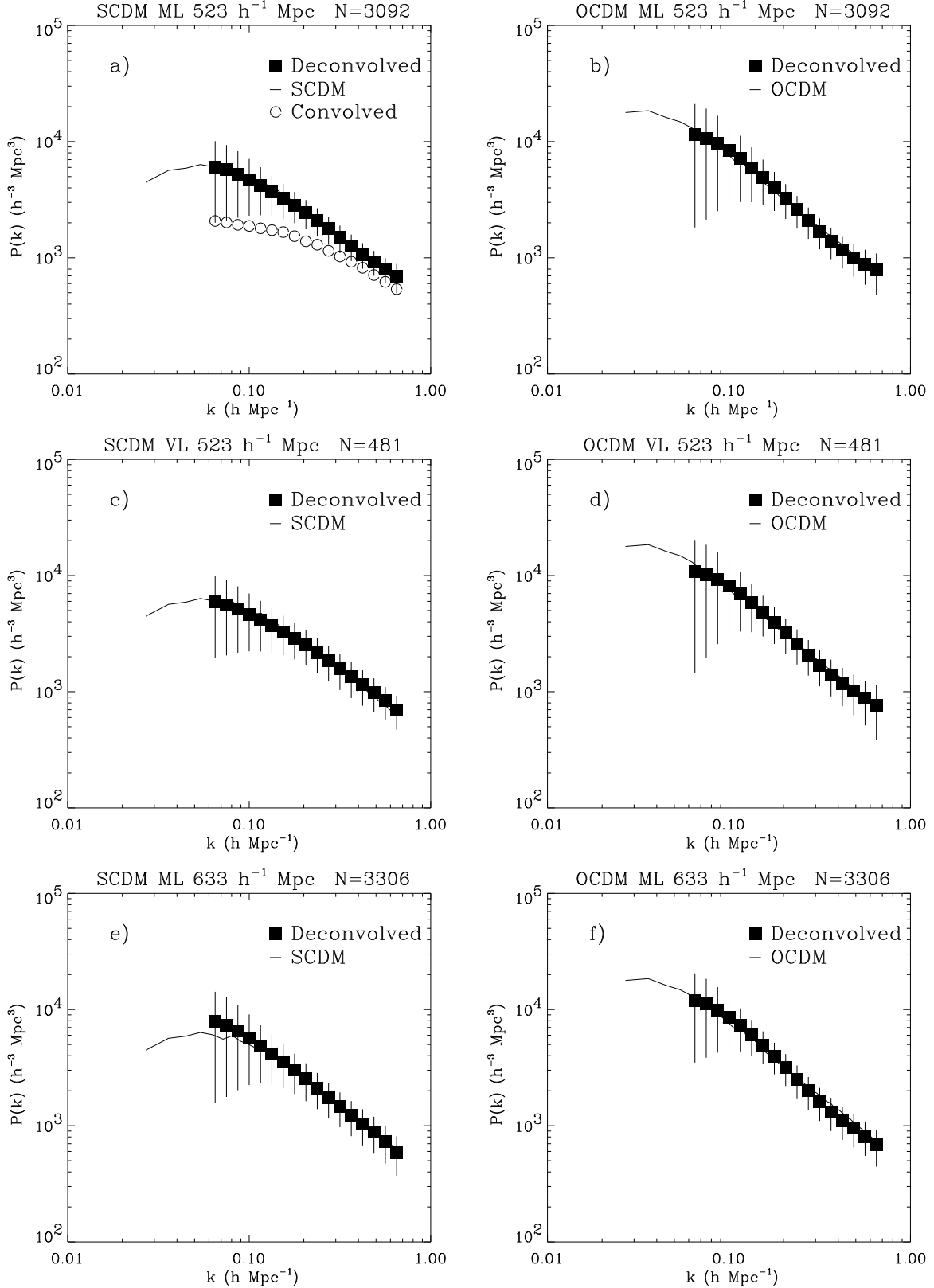


Figure 5. Deconvolved power spectra from 50 mock ESP catalogues extracted from SCDM (left panels) and OCDM (right panels) simulations. The filled squares and the error bars give the ensemble average and standard deviation of the 50 mock samples. The solid line is the corresponding power spectrum computed from the whole simulation box using all particles. N denotes the average number of particles among the mock catalogues. The three pairs of panels, from top to bottom, refer to the three different kinds of subsamples ESPm523, ESP523, and ESPm633, as in the case of the real data. In panel a) we plot also the power spectrum estimate before applying the deconvolution procedure (open circles).

due to the strongly anisotropic shape), the power is spread over a wide range of wavenumbers.

4 NUMERICAL TESTS

We test the whole procedure for estimating the power spectrum by means of N -body simulations that we have run assuming some cosmological models (Carretti 1999). The results of these simulations can be considered as a Universe, from which we can extract mock catalogues with the same features of the ESP survey (geometry, galaxy density, field completeness, selection function). We then apply to such mock catalogues the whole power spectrum estimate procedure (convolved power spectrum estimator and deconvolution technique) and we compare the result with the *true* power spectrum obtained from the whole set of particles.

The simulations were performed on a Cray T3E at CINECA supercomputing center (Bologna) using a Particle-Mesh (PM) code (Carretti & Messina 1999) and adopting two cosmological models: an unbiased Standard Cold Dark Matter (SCDM: $\Omega_0 = 1$, $h = 0.5$, $\sigma_8 = 1$) and an unbiased Open Cold Dark Matter with shape parameter $\Gamma = 0.2$ (OCDM: $\Omega_0 = 0.4$, $h = 0.5$, $\sigma_8 = 1$). They were run with a box size of $700h^{-1}$ Mpc, 512^3 grid points and 512^3 particles, in order to reproduce a volume which can contain all catalogues selected for the analysis (max depth $633h^{-1}$ Mpc) and to select a realistic number of mock galaxies for the magnitude-limited catalogues. From each simulation box, we randomly choose a particle as origin and extract sets of particles with the same features of the three ESP catalogues. The magnitude-limited selection is then reproduced by simply assigning a weight corresponding to the observed selection function.

From each simulation and for each ESP subsample we construct 50 independent mock catalogues. The average number of particles over the 50 realisations is set to the number of galaxies observed in the corresponding true ESP catalogue. The power spectrum estimator is then applied to each of the 50 mock galaxy catalogues, producing an independent estimate of $P(k)$ for that specific model and sample geometry. From each set of realisations, a mean $P(k)$ and its standard deviation can finally be computed and compared to the true power spectrum obtained from all the particles.

A general result from this exercise is that for $k > 0.065h$ Mpc $^{-1}$ the systematic power suppression by the window function convolution is properly corrected by our procedure, i.e. we are able to fully recover the input $P(k)$. In figure 5 we show the reconstructed power spectra from the three sets of mock catalogues, compared to the “true” ones, both for the SCDM and OCDM simulations. In panel a), in particular, we also show (open circles) the raw power spectrum before applying the Lucy deconvolution, to emphasize the dramatic effect of the ESP window function on all scales. It is evident that for $k > 0.065h$ Mpc $^{-1}$ the mean deconvolved power spectra are a very good reconstruction of the original ones. In particular, in the SCDM case where the spectrum turnover scale is well sampled by the simulation box, the technique is able to nicely follow the change of shape at small k ’s. This is important, because guarantees that the deconvolution method has enough resolution as to follow possible features in the data power spectrum,

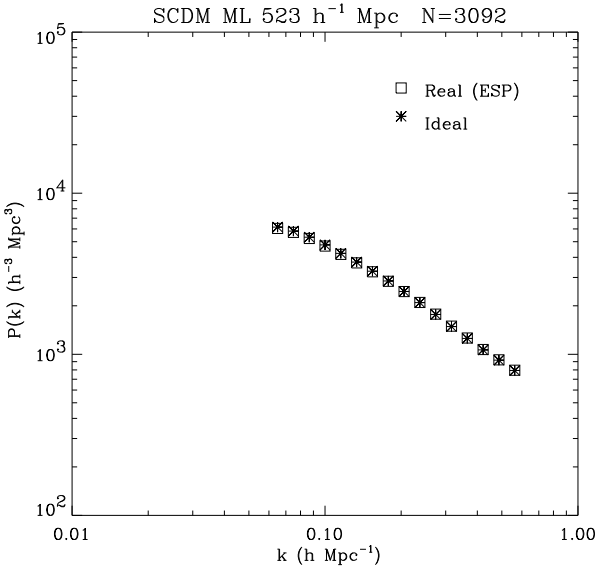


Figure 6. Test for the effect of redshift incompleteness. The power spectrum obtained has been computed for 50 mock samples extracted from the SCDM simulation, both in the ideal case of a full redshift coverage of a sample as ESPm523, and in the real situation, i.e. including the field-to-field incompleteness and correcting for it through the weighting scheme.

while at the same time recovering the correct amplitude. At smaller k ’s the error bars explode, and the results become meaningless. In the case of the deepest sample, ESPm633, the reconstruction shows a small systematic overestimate of the amplitude for the SCDM spectrum on the largest scales, i.e. the reconstruction algorithm seems to have difficulty in following the curvature of the spectrum accurately. This is probably due to the rather small value of the selection function in the most distant part of the sample, which puts too large a weight (given by its inverse) on the distant objects. Rather than indicating a difficulty in the technique, this is an indication that it is probably safer to truncate the data at smaller distances, as for the case of ESPm523.

Comparing the results from the SCDM and OCDM mock catalogues, one sees that the relative error bars for the two cases are quite similar. Not knowing *a priori* the correct cosmological model, a reasonable choice for the errors on our estimates of the ESP power spectrum is possibly provided by the average of the relative errors from the two models. Note that in this way we also include the effect of cosmic variance (clearly under the assumption that the true power spectrum has not a dramatically different shape at very small k ’s).

Using the mock catalogues, it is also interesting to evaluate directly the possible effects of the field incompleteness on the power spectrum estimate. Figure 6 compares the mean power spectra obtained for one of the SCDM mock samples both in the ideal case (all fields complete) and when the ESP field-to-field incompleteness is introduced and corrected for. It is clear that the incompleteness is correctly taken into account by the weighting scheme. Error bars (not reported for clarity) are also very similar.

5 THE POWER SPECTRUM OF ESP GALAXIES

The numerical tests performed have given us an estimate of the reliability of our method to reconstruct the true power spectrum, so that we can now apply it to the three galaxy subsamples ESPm523, ESP523 and ESPm633. The final results of the computation are shown in figure 7 and Table 2. The error bars are partially reported only for ESPm523 to avoid confusion (the errors are similar for the three samples).

Note how the three estimates of the power spectrum are quite similar, with differences among the points that are always within one standard deviation. In fact, given the large amplitude of the errors ($\sim 30\%$ of $P(k)$ for $k > 0.15h \text{ Mpc}^{-1}$, 50% for $k \sim 0.1$ and 75% for $k \sim 0.065$) the small differences in the slopes are also not significant. In general, we can safely say that the power spectrum of ESP galaxies follows a power law $P(k) \propto k^n$ with $n \sim -2.2$ for $k > 0.2h \text{ Mpc}^{-1}$, and $n \sim -1.6$ for $k < 0.2h \text{ Mpc}^{-1}$. In the range $0.065 < k < 0.6h \text{ Mpc}^{-1}$ there is no meaningful difference between the three estimates, which are therefore independent of the catalogue type (magnitude- or volume-limited) and of the catalogue depth.

In figure 7 we have also plotted, for comparison, the simple linear power spectra for two models, a standard CDM with $\Omega = 1$ and $H_o = 50$ (solid line) and a Λ -CDM with $\Omega_M = 0.3$ and $\Omega_\Lambda = 0.7$ (dashed line). Both models are normalised to COBE. Despite the comparison is deliberately simplistic, one can safely say that the data points (especially below $k = 0.2 \div 0.3h \text{ Mpc}^{-1}$, where non-linear effects are not crucial), are in much better agreement with the Λ -CDM power spectrum. This model would reproduce the observations with the only simple extra ingredient of a scale-independent bias $b \sim 1.3$.

6 CONSISTENCY BETWEEN REAL AND FOURIER SPACE

It is interesting to compare the Fourier transform of the ESP power spectrum estimated in this work with the two-point correlation function measured independently from the same sample (Guzzo et al. 2000). This exercise is a further check of the robustness and self-consistency of the estimate of $P(k)$. In addition, it is of specific interest to verify the effect of the survey geometry/window function in real and Fourier space. To simplify the procedure, we have first fitted the observed $P(k)$ with a simple analytical form with two power laws connected by a smooth turnover (e.g. Peacock 1997)

$$P(k) = \frac{Ak^\alpha}{1 + (k/k_c)^{\alpha-n}} , \quad (32)$$

where A is a normalisation factor, k_c gives essentially the turnover scale, n is the large-scale primordial index (here fixed to $n = 1$), and α gives the slope for $k \gg k_c$. We have used this function to fit both the convolved and deconvolved estimates of $P(k)$ obtained from the ESP523 sample. In terms of selection function, this sample is the closest to one of the volume-limited samples used by Guzzo et al. (2000) to estimate $\xi(s)$ from the same data. Figure 8 shows how this form provides a good description of the observed

ESP power spectrum, both before and after the deconvolution has been performed.

Figure 9 shows the Fourier transform of the two fits, compared to the direct estimate of $\xi(s)$ by Guzzo et al. (2000). Two main comments should be made here. First, our "best" estimate of $P(k)$, deconvolved for the ESP window function according to our recipe, reproduces very well the observed two-point correlation function (solid line). Note how the Fourier transform of the simple direct estimate suffers from a systematic lack of power as a function of scale (dashed line), as we expected from our results on the mock samples. The second comment is a more general one and concerns the stability of the two-point correlation function. One might naively think that the narrowness of the explored volume, which gives rise to the window function in Fourier space, should affect in a similar way also the estimate of clustering by the two-point correlation function. Figure 9 shows that this is not the case. In fact, the points showed here have not been subject to any kind of correction (Guzzo et al. 2000). Still, they seem to sample clustering to the largest available scales in a reasonably unbiased way, without basically "feeling" the survey geometry. In other words, it is clear that as far as the geometry of the survey is concerned, the "good old" correlation function seems to perform better than the power spectrum.

7 COMPARISON TO OTHER REDSHIFT SURVEYS

In the six panels of figure 10, we compare the power spectrum for the ESPm523 and ESPm633 samples to a variety of results from previous surveys, both selected in the optical and infrared (IRAS) bands. In general, there is a good level of unanimity among the different surveys concerning the slope of $P(k)$ over the range sampled by the ESP estimate. Optically-selected surveys show a good agreement also in amplitude, with a possible minor biasing effect in the case of CfA2-SSRS2-130 (panel a, da Costa et al. 1994), which is a volume-limited sample containing galaxies brighter than $\sim M^* - 1.5$. The effect of biasing is more clearly seen when the comparison is made with the IRAS-based surveys, as the IRAS 1.2Jy (Fisher et al. 1993), QDOT (Feldman et al. 1994), and PSCz (Sutherland et al. 1999) surveys (panels e and f).

Particularly relevant is the comparison to the results of the Durham/UKST galaxy redshift survey (DUKST, Hoyle et al., 1999) (panel d). This survey is selected from the same parent photometric catalogue as the ESP, the EDSGC, but covers a much larger solid angle, sparsely sampling the galaxy distribution to $b_J \sim 17$ by picking one in three galaxies. It is therefore essentially complementary to the ESP in geometry, while containing a comparable number of galaxies. The agreement between these two data sets is impressive. This is a further confirmation of the quality of the deconvolution procedure we have applied to the ESP data, given the rather 3D shape of the DUKST volume which makes the window function practically negligible for this survey. Significantly more noisy is the estimate from the similarly b_J -selected Stromlo-APM redshift survey (Tadros & Efstathiou 1996), most probably because of the very sparse sampling of this survey and the smaller number of galaxies.

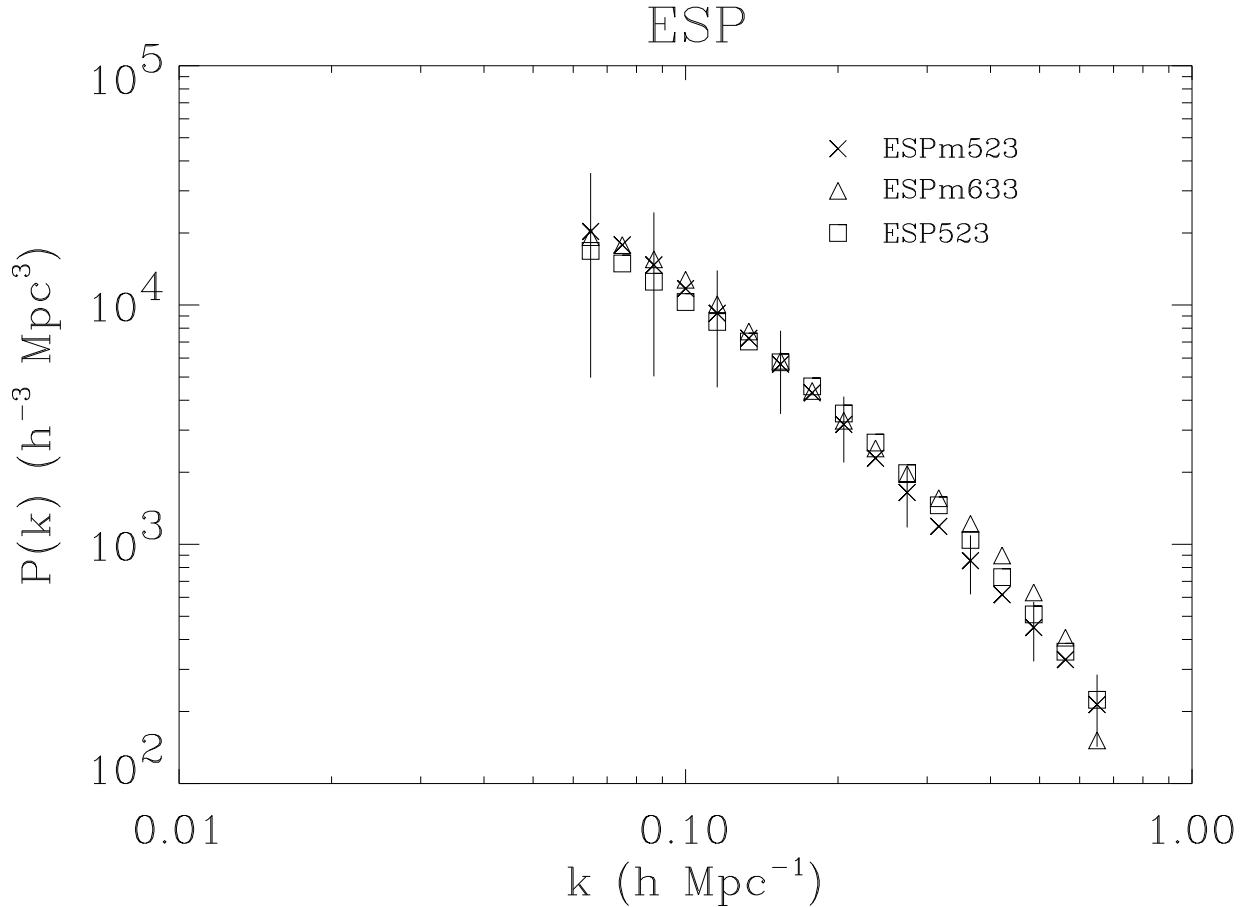


Figure 7. The final deconvolved estimates of the ESP power spectrum from the three samples. The solid and dashed line show, for reference, the COBE-normalized linear power spectra for a standard flat CDM model and a Λ -CDM model with $\Omega_M = 0.3$ and $\Omega_\Lambda = 0.7$.

Table 2. Results of the power spectrum estimates from the three subsamples of the ESP survey. Errors are estimated from 50 mock realisations of the samples, as detailed in the text.

k ($h\text{Mpc}^{-1}$)	$P(k)_{ESPm523}$	$1\sigma_{ESPm523}$	$P(k)_{ESPm633}$	$1\sigma_{ESPm633}$	$P(k)_{ESP523}$	$1\sigma_{ESP523}$
0.065	20284.1	15313.7	19215.2	14497.3	16830.1	12935.8
0.075	17831.0	12781.3	17791.6	12565.5	14907.9	10737.9
0.087	14703.1	9671.4	15515.0	9786.9	12507.9	8122.6
0.100	11714.0	6853.1	12750.5	6921.8	10288.4	5867.9
0.115	9238.4	4711.6	10077.0	4658.0	8496.4	4210.6
0.133	7263.2	3200.0	7747.6	3103.9	7035.9	3024.2
0.154	5657.4	2149.3	5847.8	2109.7	5760.2	2175.6
0.178	4295.9	1437.8	4371.9	1491.0	4568.9	1581.1
0.205	3168.1	972.4	3284.7	1092.9	3520.3	1177.4
0.237	2289.4	671.1	2514.1	827.7	2661.9	893.5
0.274	1645.7	470.0	1964.7	638.8	1983.4	674.5
0.316	1187.8	333.6	1557.9	505.0	1455.4	500.3
0.365	853.9	236.0	1216.7	395.9	1042.6	360.9
0.422	615.7	169.3	898.3	295.7	729.0	254.8
0.487	449.0	125.1	629.0	209.3	509.1	180.1
0.562	329.5	95.6	406.9	137.6	355.6	128.9
0.649	213.8	71.5	151.4	54.8	223.9	91.6

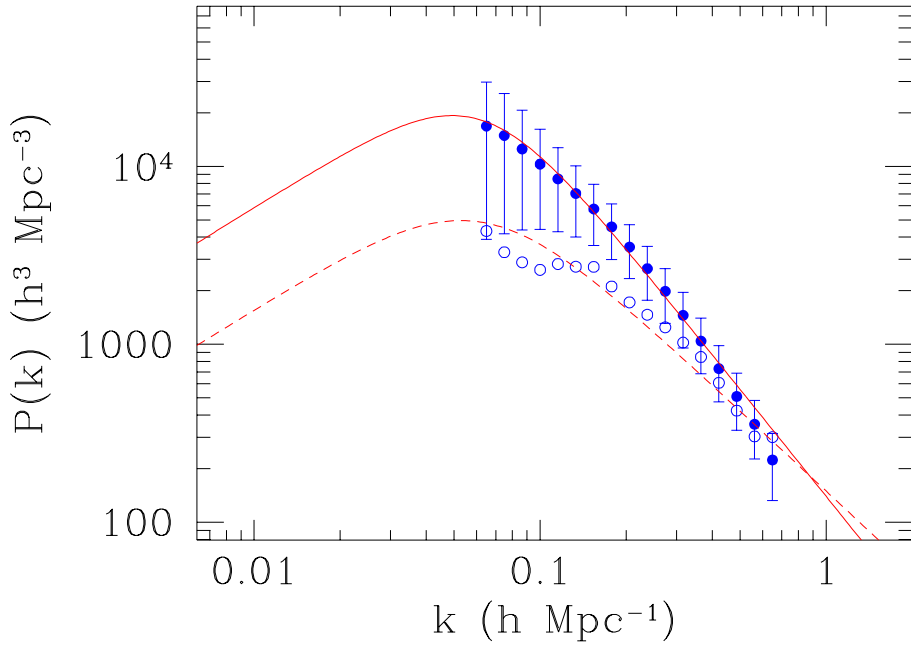


Figure 8. Fits with a simple phenomenological form of the convolved and de-convolved $P(k)$ from the ESP523 sample

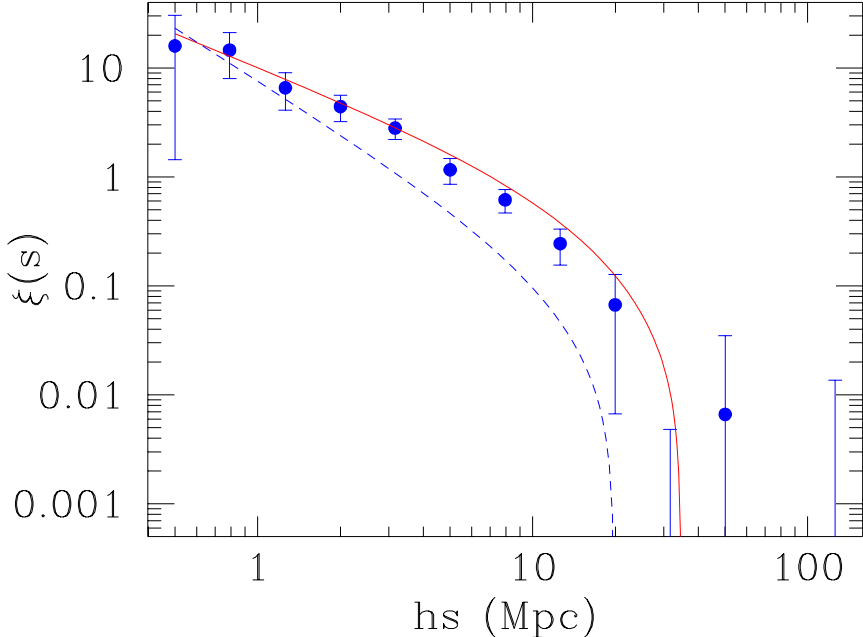


Figure 9. The Fourier transform of the convolved (dashed line) and de-convolved (solid line) estimates of the power spectrum compared to the two-point correlation function of the ESP survey (filled circles), estimated for essentially the same volume-limited subsample (Guzzo et al. 2000). The Fourier transform of the de-convolved estimate is in very good agreement with the direct measure of $\xi(s)$. This result shows also how the two-point correlation function – for which no kind of correction has been applied – is substantially insensitive to the effect of the window function.

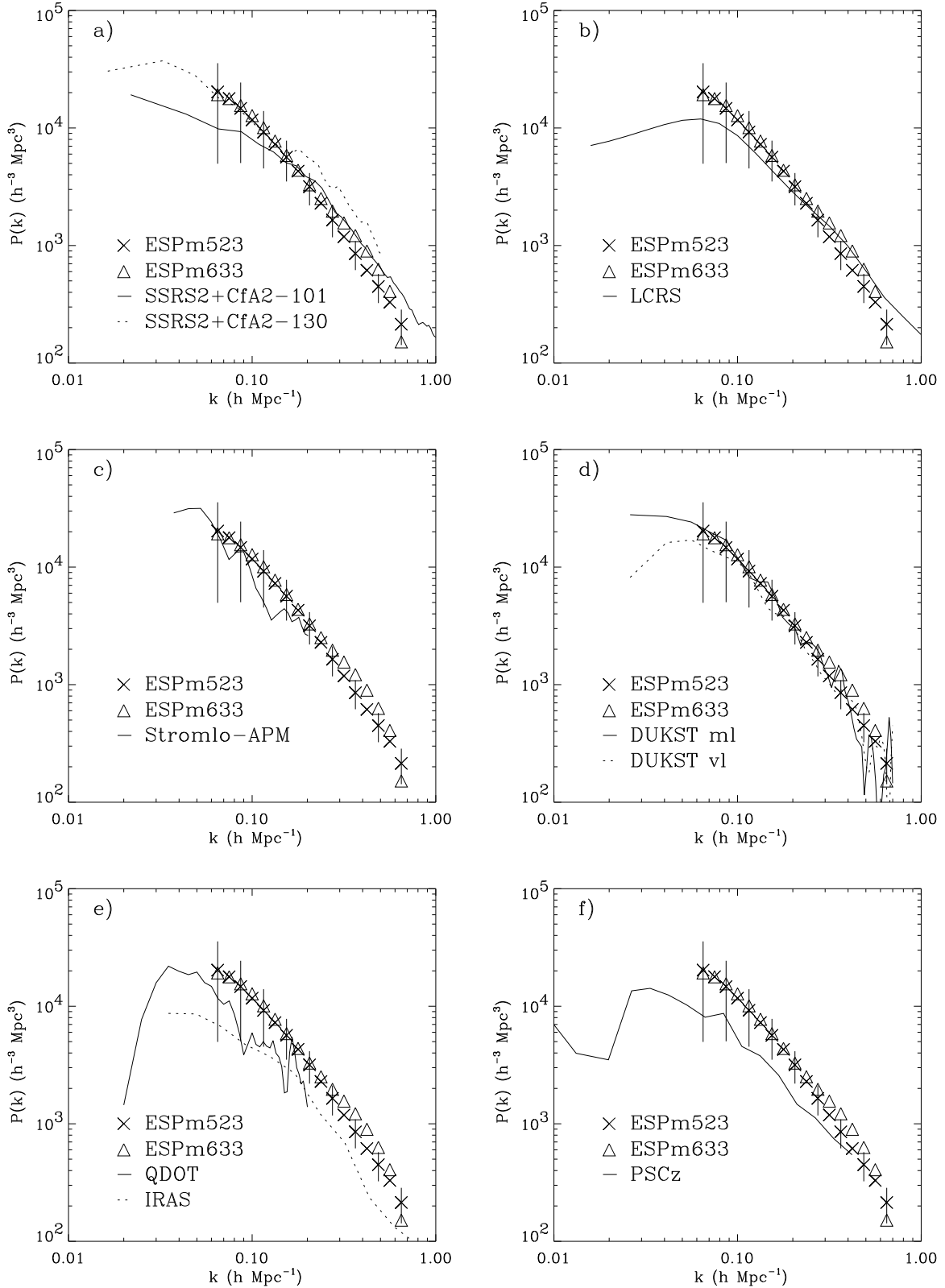


Figure 10. Comparison of two estimates of the ESP $P(k)$ with results from other surveys, as indicated by the labels (see text for references). Error bars for the ESP points are reported only partially for clarity.

Finally, panel b) shows a comparison with the data from the r -selected LCRS (Lin et al. 1996). The power spectrum from this survey has a flatter slope with respect to our estimate from the ESP. More in general, it is flatter than practically all other power spectra shown in the figure. This is somewhat suspicious, as the two-point correlation functions agree rather well for ESP, LCRS, Stromlo-APM and DUKST (Guzzo 1999), and might be an indication that the effect of the window function has not been fully removed from the estimated spectrum.

8 SUMMARY AND CONCLUSIONS

In this paper we have developed a technique to properly describe the ESP window function analytically, and then deconvolve it from the measured power spectrum, to obtain an estimate of the galaxy power spectrum. The tests performed on a number of mock catalogues drawn from large N -body simulations show that the technique is able to recover the correct shape of $P(k)$ down to wavenumbers $k \simeq 0.065 h \text{ Mpc}^{-1}$. In general, this technique for describing the window function analytically can be applied to any redshift survey composed by circular patches on the sky (e.g. the ongoing 2dF survey). In addition to its mathematical elegance, it has some computational advantages over the traditional method for recovering the survey window function, normally based on the generation of large Montecarlo poissonian realisations.

The final estimates of the ESP power spectrum, extracted from three subsamples of the survey, are in good agreement within the error bars, with the bright volume-limited sample not showing a clear difference in amplitude with respect to the apparent-magnitude limited ones. This agrees with the similar behaviour found for the two-point correlation function, i.e. a negligible evidence for luminosity segregation even for limiting absolute magnitudes $M_{b_J} \sim -20$ (Guzzo et al. 2000). This is only apparently in contrast with the results of Park et al. (1994), who found evidence for luminosity segregation studying the amplitude of the power spectrum in the CfA2 survey. In fact, that analysis concentrates on a range of luminosities about one magnitude brighter than M^* , which for the CfA2 survey has a value of -18.8 (Marzke et al. 1994), i.e. nearly one magnitude fainter than for the ESP. This also agrees with the results of Benoist et al. (1996), who studied the correlation function for the SSRS2 sample, finding negligible signs of luminosity segregation for $M > M^*$.

All three estimates of $P(k)$ show a similar shape, with a well defined power-law k^n with $n \simeq -2.2$ for $k \geq 0.2 h \text{ Mpc}^{-1}$, and a smooth bend to a flatter shape ($n \simeq -1.6$) for smaller k 's. The smallest wavenumber where a meaningful reconstruction can be performed ($k \simeq 0.065 h \text{ Mpc}^{-1}$), does not allow us to explore the range of scales where other power spectra seem to show a flattening and hints for a turnover. A simple comparison with the linear power spectra for two models, a standard CDM with $\Omega = 1$ and $H_0 = 50$ and a Λ -CDM with $\Omega_M = 0.3$ and $\Omega_\Lambda = 0.7$, can safely say that the data points (especially below $k = 0.2 \div 0.3 h \text{ Mpc}^{-1}$, where non-linear effects are not crucial), are in much better agreement with the Λ -CDM power spectrum. This model

would reproduce the observations with the only simple extra ingredient of a scale-independent bias $b \sim 1.3$.

We have verified that the two-point correlation function $\xi(s)$ is much less sensitive to the effect of a nasty window function as that of the ESP, than the power spectrum $P(k)$. In fact, the measured correlation function (without any correction), agrees with the Fourier transform of the power spectrum, only after this has been deconvolved for the window function. This is an instructive example of how these two quantities, despite being mathematically equivalent, can be significantly different in their practical estimates and be very differently affected by the peculiarities of data samples.

When compared to previous estimates from other surveys, the ESP power spectrum is virtually indistinguishable from that of the Durham-UKST survey, which is a sparsely sampled redshift survey covering a larger and more regular volume than the ESP, thus independently confirming the quality of the deconvolution procedure. A combination of the Durham-UKST and ESP survey seems to provide at present the best available estimate of $P(k)$ for blue-selected galaxies in the full range $\sim 0.03 - 0.8 h \text{ Mpc}^{-1}$.

ACKNOWLEDGMENTS

We thank Hume Feldman, Huan Lin, and Michael Vogeley for providing us with their power spectrum results in electronic form. LG and EZ thank all their collaborators in the ESP survey team, for their contribution to the success of the survey. This work has been partially supported by a CNAA grant.

REFERENCES

- Avila G., D'Odorico S., Tarenghi, M., Guzzo L., 1989, The Messenger, 55, 62
- Baugh C.M., Efstathiou G., 1993, MNRAS, 265, 145
- Benoist, C., Maurogordato, S., da Costa, L.N., Cappi, A., & Schaeffer, R., 1996, ApJ, 472, 452
- Cappi A. et al., 1998, A&A 336, 445
- Carretti E., 1999, PhD thesis, Univ. Bologna
- Carretti E., Messina A., 1999, in Fifth European SGI/Cray MPP Workshop, <http://www.cineca.it/mpp-workshop/fullpapers/carretti/carretti.htm>
- Colless, M., 1998, in Colombi S., Mellier Y., Raban B., eds, Proc. Wide Field Surveys in Cosmology, Edition Frontieres, Paris, p. 77
- da Costa L.N., Vogeley M.S., Geller M.J., Huchra J.P., Park C., 1994, ApJ, 437, L1
- Feldman H.A., Kaiser N., Peacock J.A., 1994, ApJ, 426, 23
- Fisher K.B., Davis M., Strauss M.A., Yahil A., Huchra J.P., 1993, ApJ, 402, 42
- Guzzo L., 1999, in Montmerle T., ed, Proc. XIX Texas Symp. on Relativistic Astrophysics, in press (astro-ph/9911115)
- Guzzo L. et al., 2000, A&A in press (astro-ph/9901378)
- Heydon-Dumbleton N.H., Collins C.A., MacGillivray H.T., 1989, MNRAS, 238, 379
- Hoyle F., Baugh C.M., Shanks T., Ratcliffe A., 1999, MNRAS, in press (astro-ph/9812137)
- Lin H., Kirshner R.P., Shectman S.A., Landy S.D., Oemler A., Tucker D.L., Schechter P.L., 1996, ApJ, 471, 617
- Lucy L.B., 1974, AJ, 79, 745

Margon, B., 1998, Phil. Trans. R. Soc. Lond. A, in press (astro-ph/9805314)

Marzke R.O., Huchra J.P., Geller M.J., 1994, ApJ, 431, 569

Mattig W., 1958, Astron. Nachr., 284, 109

Park C., Vogeley M.S., Geller M.J., Huchra J.P., 1994, ApJ, 431, 569

Peacock A.J., 1997, MNRAS, 284, 885

Peacock A.J., Nicholson D., 1991, MNRAS, 253, 307

Peebles P.J.E., 1980, The Large Scale Structure of the Universe. Princeton University Press, Princeton, NJ

Schechter P., 1976, ApJ, 203, 297

Shectman S.A., Landy S.D., Oemler A., Tucker D.L., Lin H., Kirshner R.P., Schechter P.L., 1996, ApJ, 470, 172

Sutherland W., Tadros H., Efstathiou G., Frenk C.S., Keeble O., Maddox S., McMahon R.G., Oliver S., Rowan-Robinson M., W. Saunders W., S. D. M. White S.D.M., 1999, MNRAS, in press (astro-ph/9901189)

Tadros H., Efstathiou G., 1996, MNRAS, 282, 1381

Tegmark M., Hamilton A.J.S., Strauss M.A., Vogeley M.S., Szalay A.S., 1998, ApJ, 499, 555

Vettolani G. et al., 1997, A&A 325, 954

Vettolani G. et al., 1998, A&ASS 130, 323

Zucca E. et al., 1997, A&A 326, 477

This paper has been produced using the Royal Astronomical Society/Blackwell Science L^AT_EX style file.